Fabrication and experimental evaluation of microstructured ^{6}Li silicate fiber arrays for high spatial resolution neutron imaging

Michael E. Moore[a], Joris Lousteau[b], Pavel Trtik[c], Hassina Z. Bilheux[d], Diego Pugliese[e], Daniel Milanese[e], Angela T. Simone[a], Gilberto Brambilla[b], Jason P. Hayward[a]

[a] Department of Nuclear Engineering, University of Tennessee, Knoxville, TN 37996, USA

[b] Optoelectronics Research Centre, University of Southampton, Southampton, SO17 1BJ, UK

[c] Laboratory for Neutron Scattering and Imaging, Paul Scherrer Institut (PSI), CH-5232 Villigen, Switzerland

[d] Neutron Scattering Division, Oak Ridge National Laboratory, Oak Ridge, TN 37831, USA

[e] Department of Applied Science and Technology and RU INSTM, Politecnico di Torino, Corso Duca degli Abruzzi 24, 10129 Torino, Italy

Abstract

This work presents the fabrication and experimental evaluation of instrumentation designed to enable higher spatial resolution neutron radiography for those performing research at neutron scattering facilities. Herein, we describe a proof-of-concept array of microstructured silicate fibers with ^{6}Li doped cores that shows progress towards a design for μm resolution neutron radiography. The multicore fiber was fabricated by drawing stacked unit elements of Guardian Glass (Nucsafe Inc., Oak Ridge, TN, USA), a ^{6}Li scintillating core glass, and a silicate cladding glass. These structured fibers function as an array of sub-10-μm waveguides for scintillation light. Measurements have shown a significantly increased integrated charge distribution in response to neutrons, and the spatial resolution of the radiographs is described by edge response and line spread functions of 48 ± 4 μm and 59 ± 8 μm, respectively.

Keywords: High Spatial Resolution; Lithium Glass; Multicore Fiber; Neutron Radiography; Optical Waveguides; Particle Tracking.

1. Introduction

The properties of novel X-ray opaque materials, like those used in energy storage systems, precision manufacturing technologies, aerospace components, and metallic additive manufacturing, are often described using simulation tools lacking experimentally grounded models, and are based on first-principle calculations and theoretical assumptions alone. Thus, ongoing material characterization relies on neutron scattering instrumentation to verify performance predictions and add structure to future models. Despite the successes that neutron scattering science facilities have achieved in recent years, even higher-impact research into microstructure evolution, thermodynamic, and mechanical properties of advanced materials is sometimes limited by the current spatial resolution of neutron sensing instrumentation.

Recent improvements in neutron sensing instrumentation have enabled a few modern neutron scattering facilities to reach the current state-of-the-art spatial resolution of approximately 10-25 μm [1] [2]. However, progress towards μm resolution remains a challenging goal for the neutron imaging community for two primary reasons.

Firstly, thermal neutron fluxes at even the most novel user facilities are much lower than similar X-ray imaging sources. For example, the raw power of several tens of W/cm^2 is regularly reported at advanced X-ray sources like Advanced Photon Source (APS) at Argonne National Laboratory. This power corresponds to a range of fluxes that conservatively start several orders of magnitude greater than the estimated novel thermal neutron flux of approximately $1.2 \times 10^9\ n/s/cm^2$ at the ODIN neutron imaging beamline planned at the European Spallation Source (ESS) [3].

Secondly, the efficiency of thermal neutron sensitive scintillators is in competition with the spatial resolution. Thick scintillators (mm scale) have higher efficiencies and, therefore, can produce high contrast radiographs in less time than thin scintillators (μm scale). However, a thick scintillator will have poor spatial resolution, as the position of captured neutrons is smeared throughout the scintillating volume. Conversely, thin scintillating screens and films bypass spatial resolution smearing by reducing the thickness of scintillating medium at the cost of efficiency. Still, the spatial resolution of unstructured thin scintillators is fundamentally limited by the variance introduced by the difference in track orientations of the charged particles emitted from neutron captures and the succeeding isotropic emission of scintillation light from neutron converters such as $^{6}\mathrm{Li}(n,\ ^{3}H)$, $^{10}\mathrm{B}(n,\alpha)$, and $^{157}\mathrm{Gd}(n,\gamma)$. Thus, there is a clear need to marry the benefits of high efficiency and spatial resolution while also overcoming the neutron capture position uncertainty that results from charged particle track variance. Some of our prior work based upon Monte Carlo simulation suggests that tracking these charged particles on an event-by-event basis could allow one to overcome this limiting uncertainty [2] [4].

Not long after the seminal work on neutron scintillating glasses [5] was published, scintillating fiber optic glass faceplates were being researched for particle tracking applications in high energy physics experiments in 1983 [6]. Three years later, the first results of a neutron scintillating fiber (SCIFI) tracker were reported [7]. In 1994, the first neutron radiograph, of a pierced sheet of Gd, taken using a SCIFI array was published with resolvable features on the order of several 100s of μm [8]. Since that time, SCIFIs have been researched for remote radiation dosimetry and neutron sensitive fusion applications [9] [10] [11]. More recently, interest surrounding coupling optical fiber tapers to existing scintillator based neutron imaging setups has grown with novel 11 μm resolution results [1]. However, in the last 24 years, it appears that no work has been done to build upon the original concept of the SCIFI tracker.

We propose the use of microstructured scintillating optical fiber arrays, capable of heavy charged particle (HCP) tracking via waveguiding scintillation light following neutron capture, for high resolution neutron imaging. Specifically, we utilize the well-known capture reaction for Li-glass ^{6}Li (n, α), emitting alpha (α) and triton $({}^3H)$ particles back-to-back that ionize primary and secondary electrons, exciting a Ce^{3+} activator, which in turn emits scintillation light at 395-432 nm in the near-UV/visible wavelength range. This light is transported through the neutron sensitive microstructured waveguides and is observed by a photodetector, see Figure 1. Provided that the collected and converted light has a sufficient signal to noise ratio (SNR), one should be able to observe the tracks of these particles and precisely estimate the locations of neutron capture reactions [4].

In our first generation proof-of-concept array, we attempted to use air capillaries in the cladding layer to maximize the refractive index difference between the Li-doped glass core and the cladding. While the lead oxide cladding glass was mechanically compatible with the Li core glass, the air capillaries tended to collapse, so we moved to an all-solid glass design. With the all-solid design, we have made several attempts to better match the thermal fiber pulling properties with the optical properties to achieve the best active scintillating volume and refractive index difference insofar as possible. This work describes the fabrication and characterization of this next generation, proof-of-concept neutron SCIFI tracker.

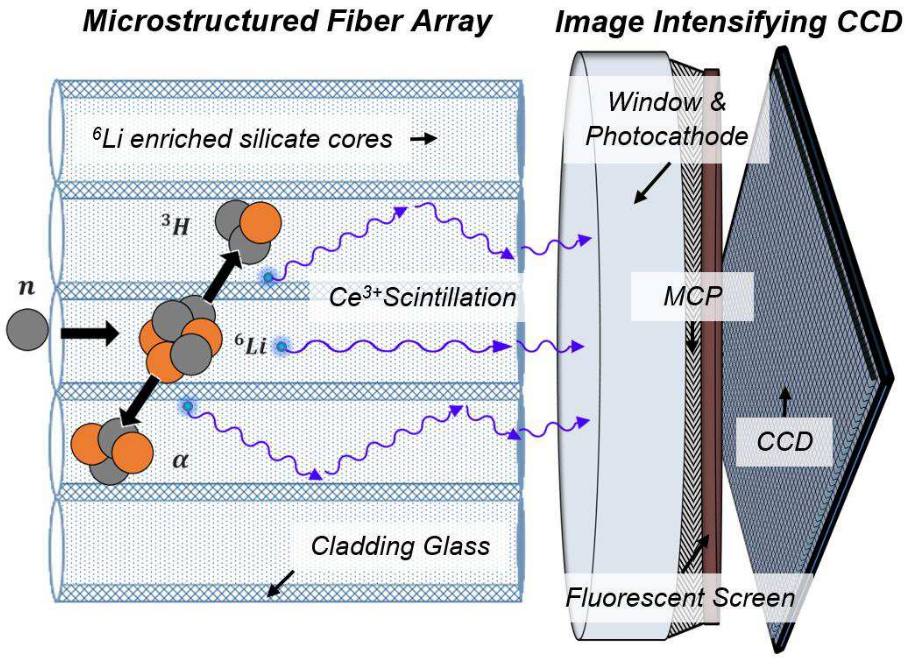

Figure 1. Enriched lithium-6 glass fibers that are doped with cerium absorb thermal neutrons, emit scintillation light, and act as optical waveguides to channel the scintillation light for imaging. They are surrounded by a cladding of lower refractive index. While an image intensifying CCD is our selected choice for a photosensor in this proof-of-concept study, it is possible that a different photosensor may be more appropriate in order to scale to a larger area.

2. Fabrication

To fabricate the neutron SCIFI, a multicore design was used. A rod of ^{6}Li-loaded glass with properties similar to GS20 [5] (fabricated by Nucsafe Inc., Oak Ridge, TN, USA) was inserted in an extruded optical glass cladding tube. Canes of Li-glass cores, embedded in the optical cladding glass, were drawn and then stacked into an array of some geometry. This array of canes, the preform, was pulled into a single multicore fiber. For this neutron SCIFI to act as a successful waveguide, the refractive index of the core, n_{co}, must be larger than the cladding refractive index, n_{cl}. While Li-glass has $n_{co} = 1.55$, a desirable cladding candidate should have $n_{cl} \leq 1.5$ [7]. Additionally, to create a uniform and regular microstructure, the glass viscosities must be matched for fiber drawing. Previous trials of ours have led to a better understanding of difficulties associated with matching both optical and thermal properties of glass fiber while maintaining the chemical stability required for scintillation. An early attempt to create a square multicore neutron SCIFI, described in detail in [12], yielded an irregular array of cores that had a refractive index almost equal to the chosen cladding. Although drawing was possible, issues related to glass devitrification during fiber pulling significantly decreased the fiber guiding properties, undermining the neutron resolution. Alternatively, the N-FK5 SCHOTT glass makes a more attractive cladding glass with an n_{cl} equal to 1.5 and a seemingly compatible transition temperature, (T_g). However, our initial canes of Li-glass and N-FK5 crystallized during drawing due to an incompatible codrawing temperature for the glass viscosities.

The fabrication of our current multicore fiber began with the extrusion of an N-KF9 cladding tube. A cylindrical glass billet with a 29 mm diameter and 35 mm height and a stainless steel die was used during the extrusion process. A 4 kN force was applied to the die and the glass billet while the glass was held in a furnace at an onset temperature of 650℃ (true glass temperature of 620℃). Some metallic inclusions were observed inside the extruded glass. Next, the Li-glass rod (11.7 mm diameter) was inserted into a 100 mm long section of the extruded N-KF9 tube, and drawn using the preform drawing method. To determine the optimal drawing temperature, the Li-doped silicate glass, T_g, was experimentally established with differential scanning calorimetry (Netzsch DSC STA 449 F1 JUPITER). The measurement was carried out with a heating rate of 5°C/min up to 1300°C in sealed Pt/Rh pans using ~ 30 mg of fine grain sample, providing a value of T_g = 470 ± 3°C. So, the fiber drawing took place at a furnace onset temperature of 800 ℃ (730 $\pm$10℃ glass temperature) under a flow of N_2 at 2 l/min. The preform was fed into the furnace at a speed of 1 mm/min, and the fiber was drawn at a speed of 5.4 m/min under a tension of 15 g. About 500 m of fiber were drawn from the preform, resulting in a fiber with an outer diameter and a core diameter of 185 ±4 μm and 150 ±4 μm, respectively.

The fiber was then cut into 2,700 separate 120-mm-long pieces and stacked as a hexagonal array. This array was then thermally consolidated into a single unit at 640℃ and the N-KF9 tube (13 ±0.2 mm OD/ 11.4 ±0.2 mm ID), used to jacket the Li-glass cores, was extruded under the same conditions previously described for the outer cladding tube. The resulting preform was then drawn into a single multicore fiber 910 ±10 µm in diameter with individual cores possessing 7–10 µm diameters, see Figure 2. The hexagonal circle packing geometry allows for the highest fill fraction (active scintillating volume) of circles (cores) to remaining space (cladding), $\frac{\pi\sqrt{3}}{6} \approx 90.7\%$, provided the pitch of cores is equal to the diameter of the cores. Given a conservative estimate of the average cladding spacing between cores of ~2 µm, we estimate that the active scintillating volume of our hexagonal multicore structure is ≈ 70%. Thus, we have found that this multicore design enables uniform core spacing at a 70% active volume, while also allowing for sub-10-µm individual core dimensions.

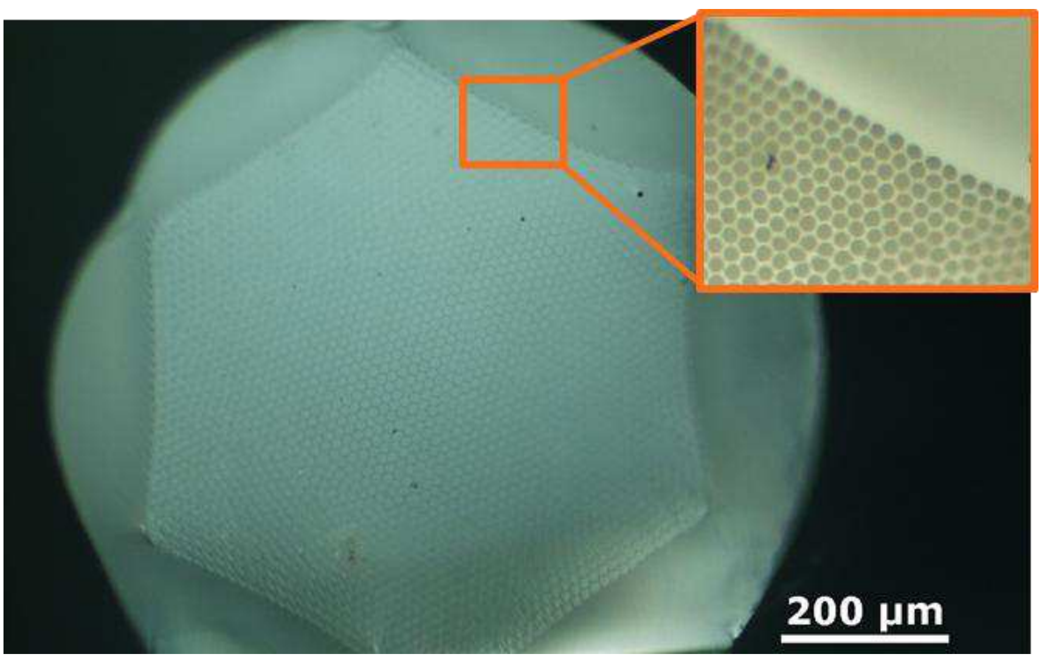

Figure 2. Photographed cross section of a cleaved end of a single multicore SCIFI (hexagonal) inside of its outer jacket (round)

3. Experimental Evaluation

Following fiber drawing, it is necessary to establish that our neutron SCIFI still scintillates as expected. Thus, the radioluminescence emission spectrum of an unpolished Li-glass rod, used for the core glass, was measured for an *On Side* (diameter) and an *On End* (length) case. The diameter of the unpolished Li glass rod was 10 mm with a length of 150 mm. A standard emission peak of Ce^{3+} scintillation light near to the 395 nm peak emission was observed for the *On Side* case, see Figure 3. For the *On End* case, the emission peak contracted 15 nm in the near-UV region. Here, the self-absorption effects of the overlapping Ce^{3+} and Ce^{4+} emission and absorption bands are observed when the scintillation light is transported further for the *On End* case. In Figure 3, these unpolished rod results are compared to the arrays of multicore SCIFIs, with and without the outer jacket removed; refer back to Figure 2 for an image of a single multicore fiber possessing an outer jacket. The SCIFI arrays were 1 mm thick with a 5 x 5 mm surface. The SCIFI arrays were measured on end, as a faceplate. After undergoing the aforementioned heat processing, the SCIFI emission behaves as expected for Ce^{3+} scintillation. The SCIFI had a slightly broadened emission, 3-5 nm, compared to the *On Side* case for the Li-glass rod.

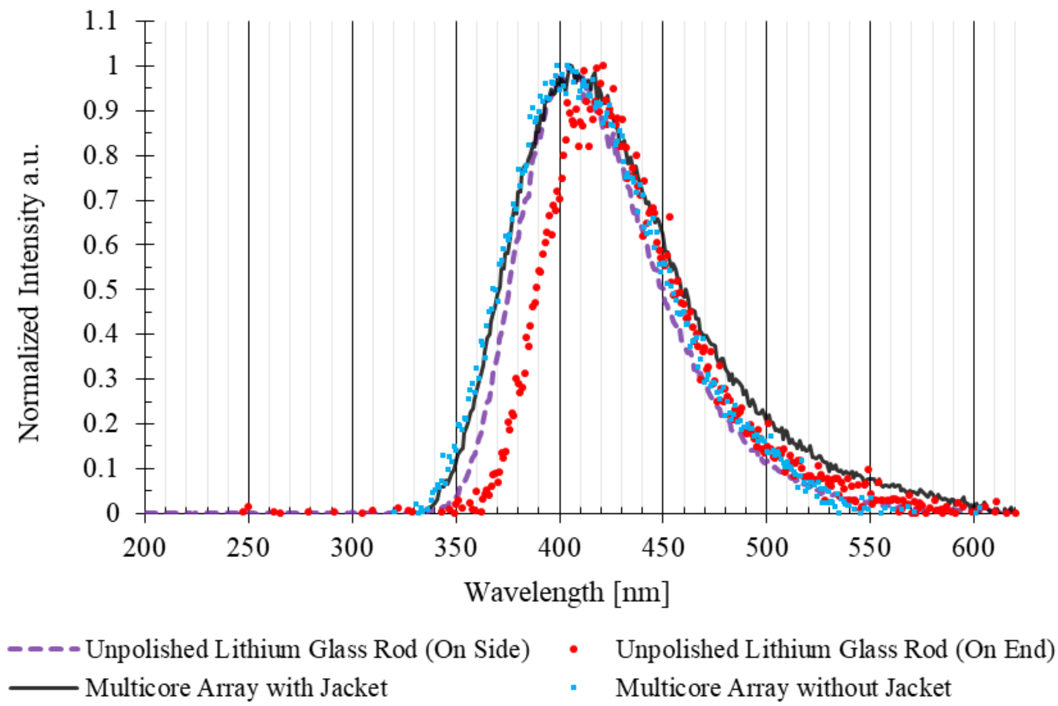

Figure 3. Radioluminescence spectra characteristic of Ce^{3+} activator emission for the unpolished ^{6}Li glass rod (unprocessed) and the multicore arrays (drawn into fibers) with and without outer jackets.

Having verified that the scintillation mechanism is behaving as expected, it is essential to characterize any transport of the Ce activator from the core to the cladding via thermal diffusion to ensure that scintillation light is being produced within the core glass. So, Energy Dispersive X-ray Spectrometry (EDS) was used to examine the atomic concentrations of dopants in cane cross-sections with a Zeiss EVO MA15 Scanning Electron Microscope. The canes of the Li-glass cores cladded with N-KF9 were embedded in epoxy, and EDS line scans were acquired across the ends of the canes. The results of the EDS line scans are shown in Figure 4, where Mg inside of the core glass can be seen as the boundary between the core and cladding. No decrease, below standard deviation, for the Ce concentration in Li-glass cores at the near-cladding position was observed. EDS point scans targeting 4 randomly selected Li-glass cores, at 3 positions each, correctly detected a Ce concentration of 2.4 $\pm$0.2 wt.%. No Ce was detected when point scans targeted the cladding with a lower detectable limit set to 0.1 wt.%. So, the intensity of the Ce concentration in the cladding and surrounding epoxy is assumed to be background.

Thus, Ce was well bound within the core glass during fiber drawing. Again, the fiber was drawn at a 730 ±10°C glass temperature, 260°C above T_g, with any given segment of fiber experiencing approximately 10 min of heating. Previous work of ours has shown that the mobility of Ce in Li-glass, heated at temperatures between 500-600°C for 5 hr with a subsequent 24 hr anneal, resulted in a few μm of Ce diffusion [13]. Thus, the quasi-immobilization of Ce for the short heating duration agrees with our experimental data.

If a significant quantity of the ^{6}Li absorber is in the SCIFI cladding, then neutron captures in the cladding could decrease overall light output, and potentially create $\pm$ 3 μm position smearing. So, it useful to know how the ^{6}Li absorber is diffusing within the multicore. However, EDS systems are fundamentally insensitive to atomic numbers < 5 due to the absorption of low energy X-rays within the detection window. X-Ray Photoelectron Spectroscopy could be used to search for Li in the cladding, but it would not provide an accurate concentration depth profile. Such a technique would require micron scale accuracy when removing core from cladding, and while probing the depth of the cladding. Instead, the mobility of another alkali metal, Na, is particularly interesting because of its chemical similarity, comparable ionic radius, and mobility to the Li absorber in the core glass. The diffusion of Na within Li enriched silicate, ^{7}Li/^{6}Li = 0.04526, and Na self-diffusion within 0.33 Na_2O, 0.67 SiO_2 glass has been shown to be closely comparable [14] [15]. Additionally, more recent analysis indicates that the activation energy for Li diffusion remains comparable to Na, specifically inside of aluminosilicate glasses; where mixed alkali effects will not immobilize Li or Na [16] [17]. The self-diffusion of Na within the cladding glass and its diffusion of 30 $\pm$4 μm into the core can be clearly seen in Figure 4. Although the EDS line scan intensities do not represent relative concentrations between elements, the Li absorber is very likely diffusing in a similar manner to Na from the core into the cladding.

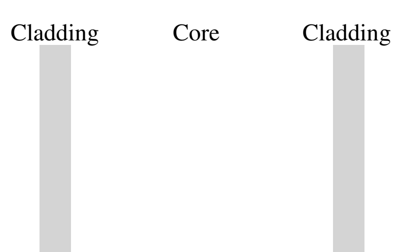

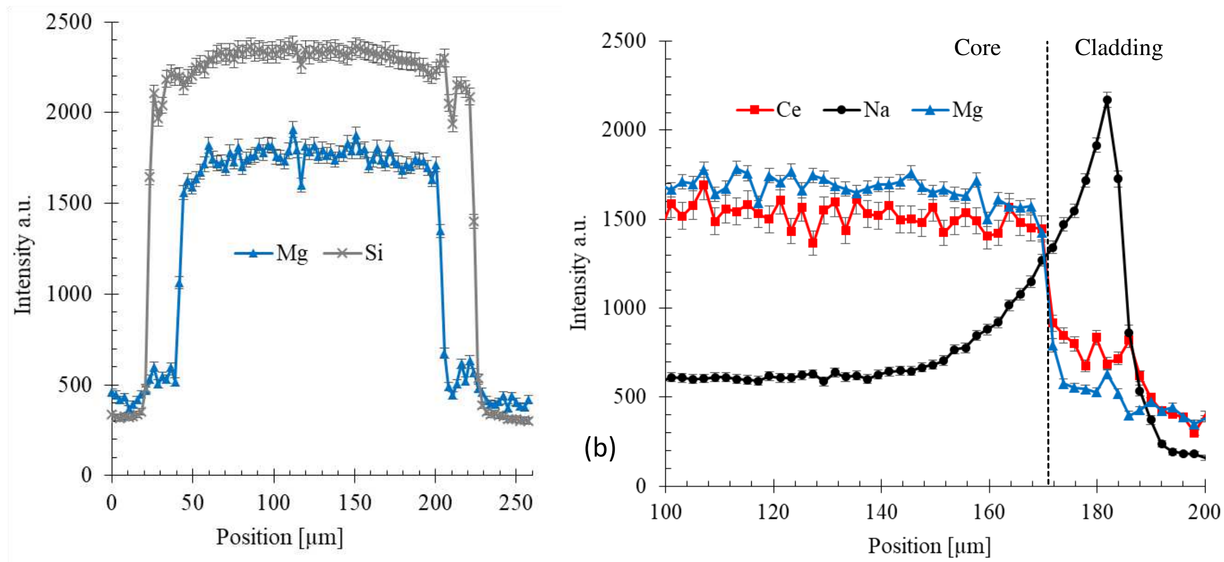

Figure 4. (a) EDS line scan across the entire cane where the core (Mg) and core/cladding (Si) components can be seen, and (b) spectra of the core-cladding interface for Mg, Ce, and Na.

Preliminary studies on gamma/neutron discrimination performance of the Li-glass within the previous square multicore SCIFI described in [12], were conducted at the CG-1D neutron imaging beamline at the High Flux Isotope Reactor (HFIR) at Oak Ridge National Laboratory (ORNL) [18]. The response of the previous square multicore SCIFI array to background radiation (cold neutron flux $< 1 \times 10^1\ n/s/cm^2$ at target with neutron shutter closed), and to the neutron beam (cold neutron flux at $\sim 1 \times 10^7\ n/s/cm^2$ at target with neutron shutter open) was observed with an R9779 PMT. The scintillation light was separable from electronic noise or Cherenkov light generated in the PMT window, both in magnitude (integrated charge) and fall time, where the longer fall times are characteristic of scintillation caused by the Ce^{3+} dopant. While scintillation was clearly seen for both cases, the response to the neutron beam displayed an increased integrated charge distribution as the array exhibited a higher light output response to cold neutrons than the gamma background radiation present in the beamline. Due to the low effective active scintillating volume of the previous square packing used (~27%), the majority of energy deposited in the multicore from the charged particles was not producing scintillation light. The current hexagonal design allows for nearly triple the amount of energy to be deposited into the scintillating core glass.

Radiographs were taken with the current hexagonal multicore fibers using the Swiss Spallation Neutron Source at the Paul Scherrer Institut (PSI). Images were acquired with the Neutron Microscope (NM) at the Pulse OverLap DIffractometer (POLDI) beamline. The use of the NM at the POLDI beamline was uniquely desired due to the requirements of the optical system needed for this experiment. Specifically, the NM possesses the magnification and numeric aperture to enable a nominal pixel size of acquired images of 1.3 µm, and a true spatial resolution of about 5 µm [19]. Additionally, the optics have µm-level repeatable positioning, and are sensitive to near UV Ce scintillation. Using the NM at the POLDI beamline is also beneficial due to a lower gamma background compared with other beamlines, a thermal/cold neutron spectrum from 1.1– 5 Å, and a flux at the sample position of $6 \times 10^6\ n/s/cm^2$ [20].

A diffused, blue light source was used to optically focus onto the ends of hand-cleaved and polished single multicore fibers. Al tape was then used to enclose the scintillator. Open Beam (OB) images were taken to focus the optics to the scintillation light. A quantity of 20 images with 300 s exposures were acquired of the OB. A gadolinium-based Siemens Star (SS) [21] was then positioned in front of the active area of the scintillator and imaged. Eighty (80) images of the SS with 300 s exposure were acquired. Due to decreased thermal neutron flux, 2 OB and 11 SS images were removed prior to post processing. The remaining SS images, with outliers removed, were divided by the OB background, and summed. The resultant image was transformed with a bilinear clockwise rotation of 90° for analysis. The resolvable spokes of the SS can be seen in Figure 5. The resolution of the 2 mm fiber can be estimated via inspection of the highlighted region of the SS spokes possessing approximately 50 µm spatial features. Referencing the 10% to 90% contrast transition for the Edge Response Function (ERF) of the spoke in the highlighted region, a 48 ±4 µm resolution was found. Fitting a Gaussian to the Line Spread Function (LSF) of the same region, a FWHM measurement yields 59 ±8 µm spatial resolution.

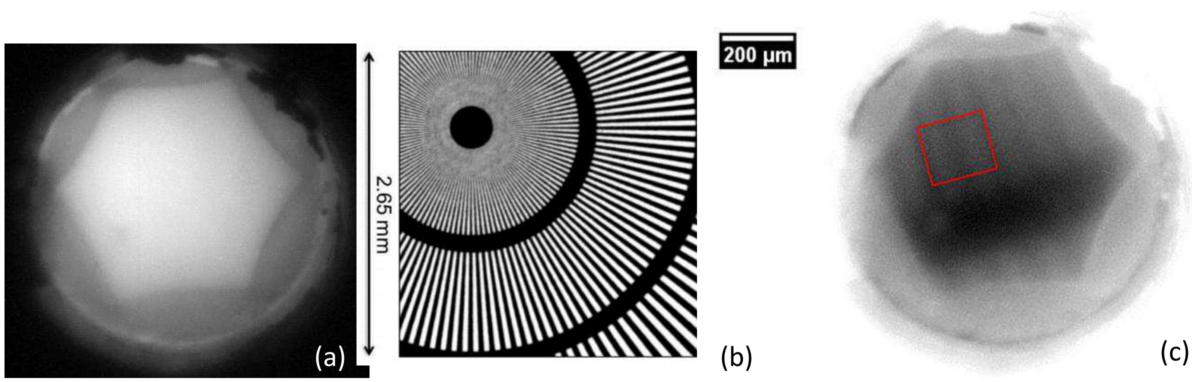

Figure 5. (a) OB neutron radiograph taken with a 2 mm thick multicore neutron SCIFI, (b) visual test object reference, PSI's Gd SS taken with the NM in [18], and (c) neutron radiograph of the SS acquired after aforementioned post processing, with the region of interest highlighted.

4. Conclusions and Future Work

Li-glass cores with 7-10 μm diameter have been drawn into 500 m of an all-solid glass composite, multicore fiber at a 70% packing fraction. The Li-glass remains active and scintillates as expected following drawing. The Li absorber shows some diffusion into the cladding, but the Ce activator is largely bound during the fabrication process. Hand-cleaved and polished single fibers of lengths 2-5 mm have resolved features on the order of 10s of μm while utilizing the Neutron Microscope. Ideal light collection in these same fibers should allow for ≤ 20 μm resolution. To increase spatial resolution, the core glass must be drawn to smaller sizes which should be possible with the current fabrication process. Image contrast improvement requires the use of a lower refractive index cladding material. Moreover, fabrication without an outer cladding jacket will allow for easy array assembly.

Near term work is planned to evaluate the radiographic spatial resolution of an array of 100 multicore neutron SCIFIs with a 5 x 5mm field-of-view. This is a comparably thinner design (1mm thick), with outer jacket removed, and it has a well-polished surface. Since a larger field-of-view was desired for evaluation of imaging performance, the multicore fiber outer jacket was ground away, and a 10×10 array was stacked together. Assembly was finished by securing the array with structural glass plate siding and polishing the surfaces, see Figure 6.

Meanwhile, a novel phosphate glass cladding, possessing a refractive index of $n_c < 1.53$, is being used for another neutron SCIFI fabrication. This cladding is expected to allow for more than twice the current amount of scintillation light to remain internally bound. We plan to draw the multicore fiber using the phosphate cladding with a goal of 2 μm diameter Li-glass cores while remaining at a packing fraction ≥ 70%.

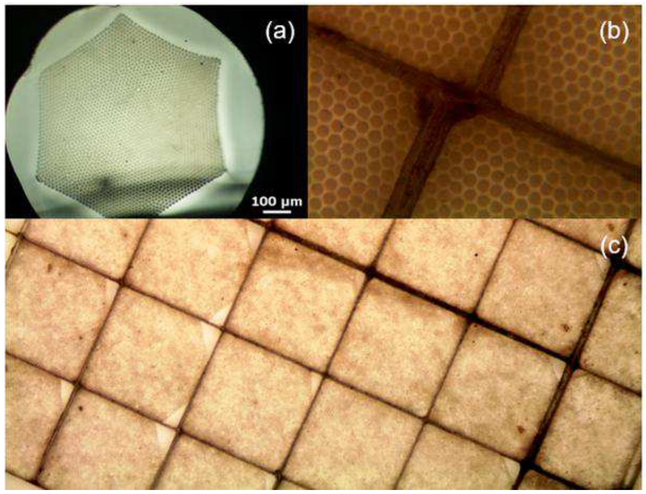

Figure 6. Microscope photos of the (a) cross section of a microstructured multicore fiber with scale, (b) stacked multicore fibers with outer cladding removed with 8 ± 1 μm core diameters, and (c) polished faceplate surface of a multicore SCIFI array with 0.5 x 0.5 mm pixels

Acknowledgements

This work was supported by the U.S. Department of Energy, Office of Science, Office of Basic Energy Sciences, under Early Career Award no. DE-SC0010314, and by the Future Photonics Hub (UK EPSRC grant EP/N00762X/1).

Experiments were performed at the Swiss spallation neutron source (SINQ), Paul Scherrer Institute, Villigen, Switzerland, and at the High Flux Isotope Reactor, a DOE Office of Science User Facility operated by the Oak Ridge National Laboratory.

This manuscript has been authored in part by UT-Battelle, LLC under Contract No. DE-AC05-00OR22725 with the US Department of Energy. The United States Government retains and the publisher, by accepting the article for publication, acknowledges that the United States Government retains a non-exclusive, paid-up, irrevocable, world-wide license to publish or reproduce the published form of this manuscript, or allow others to do so, for United States Government purposes. The Department of Energy will provide public access to these results of

federally sponsored research in accordance with the DOE Public Access Plan (http://energy.gov/downloads/doe-public-access-plan).

References

[1] M. Morgano, et al. "Unlocking high spatial resolution in neutron imaging through an add-on fibre optics taper." *Optics Express* 26.2 (2018): 1809-1816.

[2] A.S. Tremsin, et al. "Neutron radiography with sub-15 µm resolution through event centroiding." *Nuclear Instruments and Methods in Physics Research Section A: Accelerators, Spectrometers, Detectors and Associated Equipment* 688 (2012): 32-40.

[3] M. Strobl. "The scope of the imaging instrument project ODIN at ESS." *Physics Procedia* 69 (2015): 18-26.

[4] Y. Song, et al. "Monte Carlo simulation of a very high resolution thermal neutron detector composed of glass scintillator microfibers." *Applied Radiation and Isotopes* 108 (2016): 100-107.

[5] A. R. Spowart. "Neutron scintillating glasses: Part 1. Activation by external charged particles and thermal neutrons." *Nuclear Instruments and Methods* 135 (1976): 441-453.

[6] R. Ruchti, et al. "A Scintillating Glass, Fiber-Optic Plate Imaging System for Active Target and Tracking Applications in High Energy Physics Experiments." *IEEE Transactions on Nuclear Science* 30.1 (1983): 40-43.

[7] M. Atkinson, et al. "Initial tests of a high resolution scintillating fibre (SCIFI) tracker." *Nuclear Instruments and Methods in Physics Research Section A: Accelerators, Spectrometers, Detectors and Associated Equipment* 254.3 (1987): 500-514.

[8] P. Ottonello, et al. "Slow neutron imaging using scintillating glass optical fibers." *Nuclear Instruments and Methods in Physics Research Section A: Accelerators, Spectrometers, Detectors and Associated Equipment* 349.2-3 (1994): 526-531.

[9] N. Miyanaga, N. Ohba, and K. Fujimoto. "Fiber scintillator/streak camera detector for burn history measurement in inertial confinement fusion experiment." *Review of scientific instruments* 68.1 (1997): 621-623.

[10] A. Vedda, et al. "Ce 3+-doped fibers for remote radiation dosimetry." *Applied physics letters* 85.26 (2004): 6356-6358.

[11] N. Chiodini, et al. "Ce-doped SiO_2 optical fibers for remote radiation sensing and measurement." *Fiber Optic Sensors and Applications VI*. Vol. 7316. International Society for Optics and Photonics, 2009.

[12] M.E. Moore, et al. "A multicore compound glass optical fiber for neutron imaging." *Optical Fiber Sensors Conference (OFS), 2017 25th*. IEEE, 2017.

[13] M.E. Moore, et al. "Thermal diffusion of mixed valence Ce in ^{6}Li loaded silicate glass for neutron imaging." *Journal of Non-Crystalline Solids* 498 (2018): 145-152.

[14] G.H. Frischat. "Sodium diffusion in SiO2 glass." *Journal of the American Ceramic Society* 51.9 (1968): 528-530.

[15] W. Beier and G. H. Frischat. "A mass spectrometric method for the determination of Li self diffusion in oxide glasses." *Journal of Non-Crystalline Solids* 38 (1980): 569-573.

[16] W. Li, and S.H. Garofalini. "Molecular dynamics simulation of lithium diffusion in Li2O–Al2O3–SiO2 glasses." *Solid State Ionics* 166.3-4 (2004): 365-373.

[17] J.O. Isard. "The mixed alkali effect in glass." *Journal of Non-Crystalline Solids* 1.3 (1969): 235-261.

[18] L. Santodonato, et al. "The CG-1D neutron imaging beamline at the oak Ridge National Laboratory high flux isotope reactor." *Physics Procedia* 69 (2015): 104-108.

[19] P. Trtik, and E. H. Lehmann. "*Progress in High-resolution Neutron Imaging at the Paul Scherrer Institut-The Neutron Microscope Project." Journal of Physics: Conference Series,* vol. 746. No. 1. IOP Publishing, 2016.

[20] U. Stuhr, et al. "Time-of-flight diffraction with multiple frame overlap Part II: The strain scanner POLDI at PSI." *Nuclear Instruments and Methods in Physics Research Section A: Accelerators, Spectrometers, Detectors and Associated Equipment* 545.1-2 (2005): 330-338.

[21] C. Grünzweig, et al. "Highly absorbing gadolinium test device to characterize the performance of neutron imaging detector systems." *Review of Scientific Instruments* 78.5 (2007): 053708.